The Foot 40 (2019) 1–7

Contents lists available at ScienceDirect

The Foot

journal homepage: www.elsevier.com/locate/foot

Original Article

Reproducibility of radiographic methods for assessing longitudinal tarsal axes
Part 1: Consecutive case study

Masamitsu Kido[a], Kazuya Ikoma[a,*], Ryosuke Ikeda[a], Toshihiro Hosokawa[a], Yusuke Hara[a], Kan Imai[a], Masahiro Maki[a], Suzuyo Ohashi[b], Yasuo Mikami[b], Toshikazu Kubo[a]

[a] Department of Orthopaedics, Graduate School of Medical Science, Kyoto Prefectural University of Medicine, Kyoto, 602-8566, Japan
[b] Department of Rehabilitation Medicine, Graduate School of Medical Science, Kyoto Prefectural University of Medicine, Kyoto, 602-8566, Japan

ARTICLE INFO

Keywords:
Radiography
Longitudinal tarsal axes
Reproducibility
Intraobserver and interobserver correlation coefficients

ABSTRACT

Introduction: Calcaneal pitch angle and Meary's angle are commonly used to assess longitudinal foot arches on lateral-view radiographs. However, the methods used to obtain the talar, first metatarsal, calcaneal, and plantar axes differ across multiple reports, and no study has evaluated the reproducibility of these approaches. The aim of this study was to determine the most reproducible methods for radiographically evaluating longitudinal axes.
Methods: Standing radiographic images of 40 feet from 21 consecutive outpatients were obtained to measure longitudinal axes of the talus, first metatarsal, calcaneus and plantar surface, which were defined using six, five, four and three different methods, respectively, selected from previous reports. Intraobserver and interobserver correlation coefficients were calculated.
Results: The best intraobserver and interobserver correlation coefficients for the talar, first metatarsal, and calcaneal axes were obtained using methods involving a line bisecting the angle formed by the lines tangential to the superior and inferior margins of the talus, a line connecting the centre of the first metatarsal head and the midpoint of the visualized base of the first metatarsal, and a line drawn tangential to the inferior surface of the calcaneus, respectively. For the plantar axis, a method that used the horizontal plane (as a reference axis) was regarded as the best approach, although intraobserver and interobserver correlation coefficients could not be calculated because all values were zero.
Conclusions: The aforementioned methods were considered to be optimal for the radiographic assessment of longitudinal foot arches. This study could contribute to more accurate assessments of foot deformities.

1. Introduction

Various methods have been established to morphologically assess deformed feet, such as pedography [1], radiography [2–15], computed tomography (CT) [16], and magnetic resonance imaging (MRI) [17]. Although radiography involves exposure to radiation, it is comparatively inexpensive, minimally invasive, and simple, and it reflects bone alignment well. In assessing a deformed foot, the weight applied while standing best reflects the clinical condition [14]. Therefore, radiography is the most utilized assessment method during weightbearing. In assessing foot arches, radiographic images are of particular importance during weightbearing. In 1955, Davis and Hatt assessed congenital club feet to measure the angle formed by the lines through the inferior cortex of the calcaneus and the inferior cortex of the fifth metatarsal using lateral radiographic images [4]. In a 1975 textbook, Gamble and Yale described the calcaneal pitch angle formed by the weight-supporting plane and a line drawn from this plane through the anteroplantar margin of the calcaneal tuberosity to the plantar margin of the anterior portion of the calcaneus on lateral-view radiographs [6]. Since then, the calcaneal pitch angle has been commonly used to assess foot deformities. Moreover, in 1967, Meary assessed cavus feet by measuring the talar-first metatarsal angle (Meary's angle), which is the angle between the lines of the longitudinal axes of the talus and the first metatarsal in a lateral radiographic view during weightbearing [9].

Abbreviations: CT, computed tomography; MRI, magnetic resonance imaging; ICCs, intraclass correlation coefficients; PACS, picture archiving and communication system

* Corresponding author at: 465, Kajii-cho, Kawaramachi-Hirokoji, Kamigyo-ku, Kyoto, 602-8566, Japan.
E-mail address: kazuya@koto.kpu-m.ac.jp (K. Ikoma).

https://doi.org/10.1016/j.foot.2019.03.003
Received 15 November 2018; Received in revised form 26 January 2019; Accepted 11 March 2019
0958-2592/ © 2019 Elsevier Ltd. All rights reserved.

Compared with other radiographic assessment parameters, calcaneal pitch and Meary's angles have been reported to be more effective for assessing flatfoot and yield higher intraobserver and interobserver correlation coefficients [11,15]. Presently, these two angles are commonly used to assess longitudinal foot arches. However, it is difficult to determine these two angles in cases of severely deformed (i.e., flat or cavus) feet in which the tarsal bones rotate excessively. Moreover, different methods are used in the literature to establish the talar, first metatarsal, calcaneal, and plantar axes, and no study has evaluated the reproducibility of these methods. There is even confusion regarding the definitions of positive and negative Meary's angles [7,14].

The purpose of this study was to identify a radiographic method for measuring the longitudinal tarsal axes that offers the best intraobserver and interobserver correlation coefficients and to establish an ideal assessment method for deformed feet, using consecutive outpatients as subjects.

2. Materials and methods

This study was approved by the institutional review board at our hospital, which waived the requirement for informed consent (ERB-C-870). Twenty-one consecutive patients were enrolled; a total of 40 feet (10 feet from 6 men and 30 feet from 15 women; mean age, 60.4 years [SD 16.1 years]) were examined at the Department of Foot Surgery outpatient facility of this hospital in December 2016. Young patients with apparent epiphyseal lines and patients with evident wounds, autoimmune diseases such as rheumatoid arthritis, hormonal abnormalities, haemophilia, neurological disorders, and congenital abnormalities were excluded. Obviously deformed feet, including severely flat or cavus feet, were also excluded. The senior author (KI), a foot and ankle surgeon with 20 years of experience, detected foot deformities by inspection. The sample size was determined according to a previous study [11].

Foot radiography was performed at a source-to-image distance of approximately 100 cm with the patient in a standing position on both legs with the knees in full extension. The patients were radiographed barefoot with their feet straight and in a neutral position. The cassette was positioned vertically with respect to the floor. The medial border of the foot was placed on the cassette.

2.1. Definition of each measurement method

The declination angles of the talus and first metatarsal and the inclination angles of the calcaneus and plantar surface in relation to the horizontal axis were measured using six, five, four and three different methods, respectively, obtained from previous reports (Figs. 1–4) [2,3,5–13,18,19]. In cases in which there was a clear definition in the literature, that definition was used. If there was no clear definition, related articles about the measurements were discussed with the senior authors, and the definition of the measurement was clarified.

Talar axis (Fig. 1): in Method A [7], a dot is placed at the back of the articular margin of the talus (point a), another dot is placed at the middle of the nose of the talus (point d), and a line is then drawn between these dots and continued distally through the foot (textual quotation, partially rephrased); in Method B [12], the axis of the talar neck can be drawn as the line bisecting the angle formed by the lines tangential to the superior and inferior margins of the talus (textual quotation); in Method C [3], the axis is created by connecting the midpoints of lines bc (the margins of the articular surface of the talus) and ef (the margins of the neck of the talus) (textual quotation, partially rephrased); in Method D [13], the long axis of the talus is defined by connecting the midpoints of lines bc and hi (the margin of the top of the talus and the intersection point of a line perpendicular to this line and the inferior cortex of the talus); in Method E [18], the long axis of the talus is drawn from the midpoint of the height of the talar body through the mid-diameter of the talonavicular joint (textual quotation); and in Method F [2], the axis is drawn using two points equidistant from the cephalad and caudad margins of the body and the neck of the talus (textual quotation, partially rephrased). First metatarsal axis (Fig. 2): in Method G [3], the long axis of the first metatarsal is created by connecting the midpoints of lines bc (distal dorsal and plantar margins of the diaphysis of the first metatarsal) and de (proximal dorsal and plantar margins of the diaphysis of the first metatarsal) (textual quotation); in Method H [12], the mid-shaft axis of the first metatarsal is drawn as the line parallel to its superior cortical margin and extended through the centre of the metatarsal head (textual quotation); in Method I [10], the longitudinal axis of the first metatarsal is defined as a line connecting the centre of the proximal articular surface with the centre of the distal end of the diaphysis (textual quotation); in Method J [7], a dot is placed distally at the middle of the first metatarsal head, and a second dot is placed at the midpoint of the visualized base of the first metatarsal (textual quotation); and in Method K [18], the long axis of the first metatarsal is obtained by finding the diaphyseal centres at both the proximal and distal shaft levels (textual quotation). Calcaneal axis (Fig. 3): in Method L [12], the longitudinal axis of the calcaneus is drawn tangentially to the inferior surface of the calcaneus (textual quotation); in Method M [3], the line cd is used, where point c is the plantar prominence of the calcaneus proximal to the calcaneocuboid

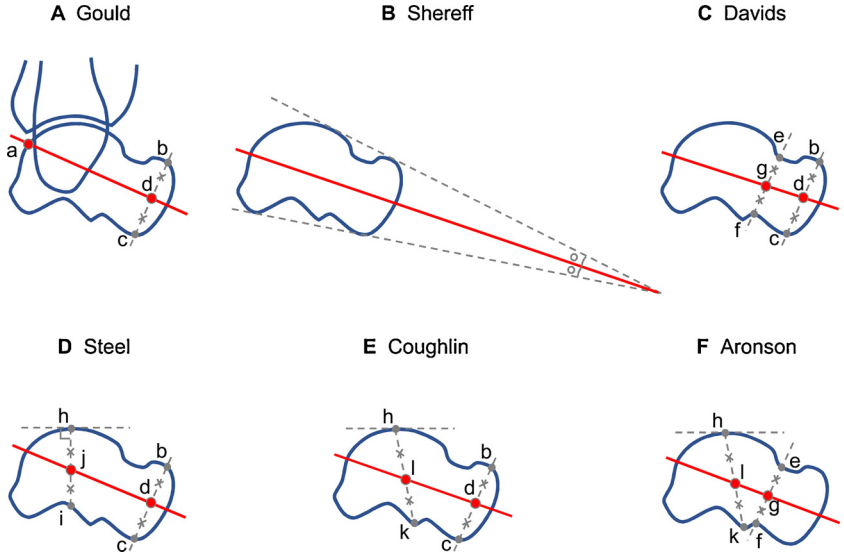

Fig. 1. Talar axes. A: point a is the back of the articular margin. Point d is the middle of the nose. B: line bisecting the angle formed by lines tangential to the superior and inferior margins. C: axis connecting midpoints of lines bc and ef. D: axis connecting midpoints of lines bc and hi. E: axis connecting midpoint of the height of the body through the mid-diameter of the talonavicular joint. F: axis connecting two points equidistant from the cephalad and caudad margins of the body and neck.

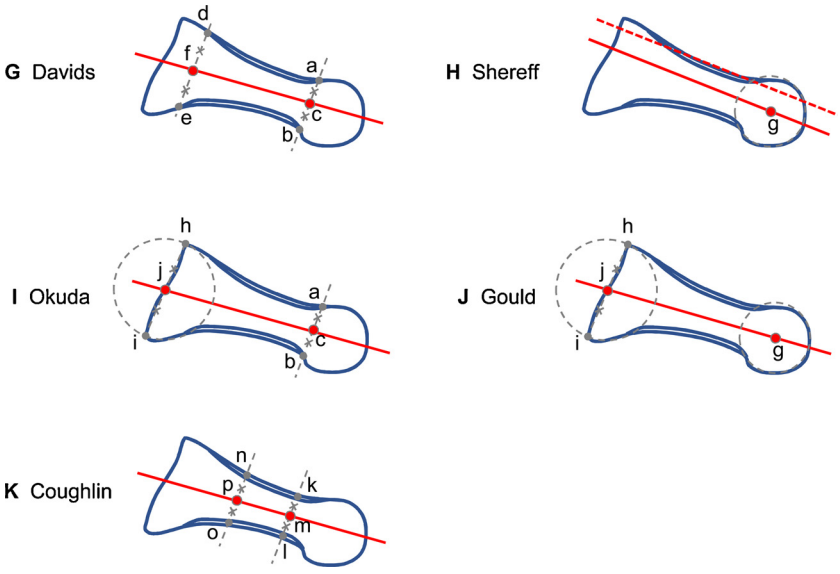

Fig. 2. First metatarsal axes. G: axis connecting midpoints of lines ab and de. H: line parallel to the superior cortical margin and extended through the centre of the head. I: line connecting the centre of the proximal articular surface with the centre of the distal end of the diaphysis. J: point g is the middle of the head. Point j is midpoint of the visualized base. K: axis connecting the diaphyseal centres at both the proximal and distal shaft levels.

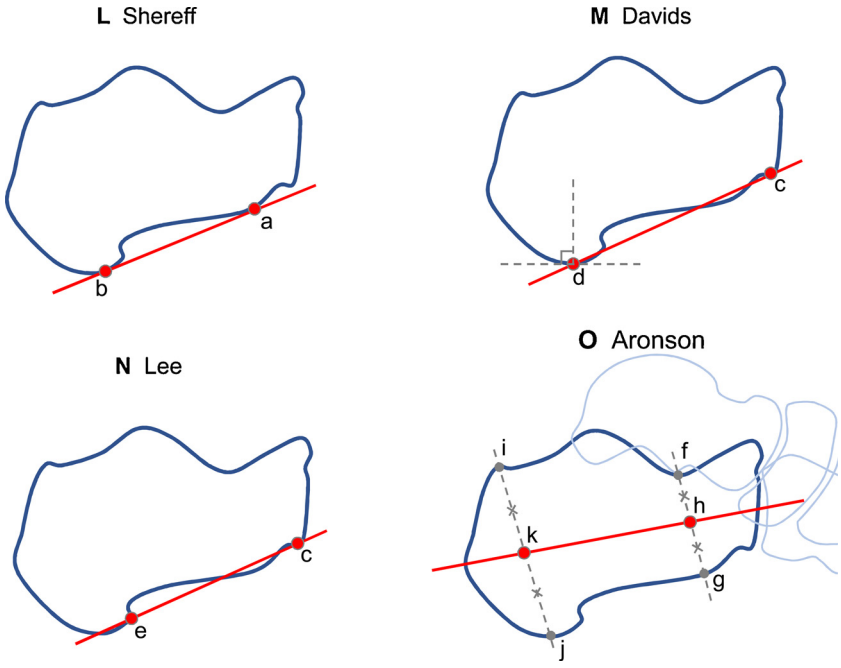

Fig. 3. Calcaneal axes. L: axis tangential to the inferior surface. M: point c is plantar prominence of the calcaneocuboid articular surface. Point d is most plantar prominence of tuberosity. N: axis drawn from the most anterior plantar point of the tubercle to the most anterior plantar point at the calcaneocuboid joint. O: axis drawn through midpoint k at the posterior tuberosity and midpoint h at the sustentaculum.

articular surface and point d is the plantar aspect of the calcaneal apophysis or the most plantar prominence of the tuberosity of the calcaneus (textual quotation, partially rephrased); in Method N [8], a line is drawn from the most anterior plantar point of the calcaneal tubercle to the most anterior plantar point of the calcaneus at the calcaneocuboid joint (textual quotation); and in Method O [2], a line is drawn along the longitudinal axis through midpoint k at the posterior tuberosity and midpoint h at the sustentaculum (textual quotation, partially rephrased). Plantar axis (Fig. 4): in Method P [3,8,10–12,19], a line is drawn from the plantar surface of the foot or the floor (textual quotation); in Method Q [5], a line is drawn from the plantar surface of the calcaneus to the inferior surface of the fifth metatarsal head (textual quotation); and in Method R [20], a line is drawn between the plantarmost points of the heel and the metatarsal heads (textual quotation).

2.2. Calculation of intraobserver and interobserver reliabilities

Intraobserver and interobserver reliabilities were calculated for the different methods using intraclass correlation coefficients (ICCs). The measurement values were obtained using the various measurement methods for each axis. Moreover, applying the optimum measurement methods, the values for calcaneal pitch and Meary's angles were calculated. All radiographic measurements were performed using picture archiving and communication system (PACS) software (IntelliSpace PACS Enterprise R4.4, Amsterdam, Netherlands). Horizontal axes were fixed and set as the reference axis (0°) in each case using the same digital goniometer. Flexion was considered positive for the assessment of the axis of the talus and first metatarsal, while dorsiflexion was considered positive for the assessment of the axis of the plantar surface, calcaneal base and calcaneus. Bony spurs were omitted for the assessments. The calcaneal pitch angle was defined as positive degrees for the dorsal angle and negative degrees for the plantar angle, according to the Shereff measurement [12]. Meary's angle was defined as positive degrees for the dorsal angle and negative degrees for the plantar angle, according to the Gould measurement [7].

The measurements were performed by 2 orthopaedic surgeons (SO

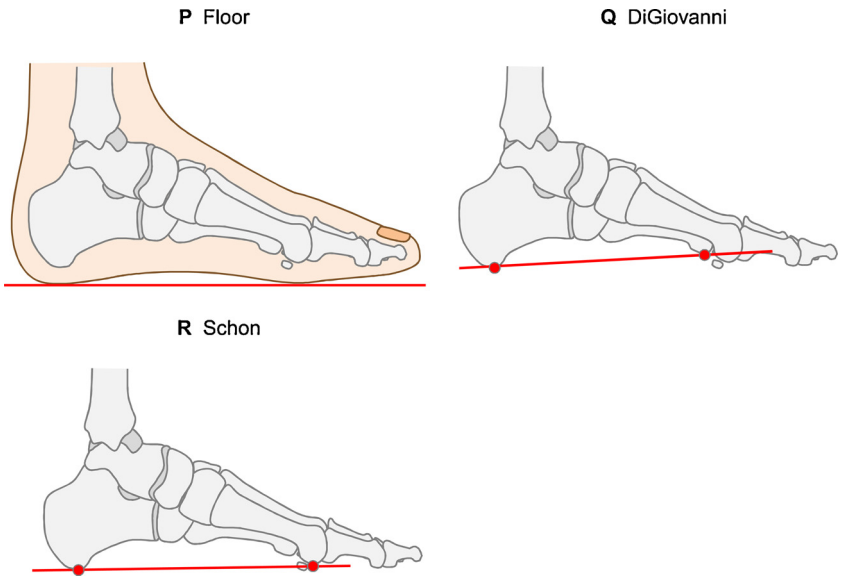

Fig. 4. Plantar axes. P: axis drawn from the plantar surface of the foot or the floor. Q: axis drawn from the plantar surface of the calcaneus to the inferior surface of the fifth metatarsal head. R: axis drawn between the most plantar points of the heel and the metatarsal heads.

and MK) who specialized in foot and ankle surgery and 1 orthopaedic surgery resident (TH), with 20, 12, and 7 years of experience, respectively. Each observer attended a lecture about the definitions and was presented with the related articles to read prior to participating in the study. Measurements of blinded radiographic images were performed in a random order using the same type of personal computer monitors (size: 21.5 inches, resolution: 1920 × 1080) and the same digital goniometer. The measurements were repeated 3 times at intervals of at least 1 week. Intraobserver and interobserver correlation coefficients were calculated and compared. For the statistical analysis, R was used (R Core Team (2016). R: a language and environment for statistical computing. R Foundation for Statistical Computing, Vienna, Austria). Based on the report by Altman, an ICC of 0.81–1 was considered very good, 0.61–0.8 good, and 0.41–0.6 moderate [21]. Post hoc power analysis under testing the null hypothesis of ICC = 0.6 was also estimated using R, and the level of significance (p value) was set at 0.0083 in the talar axis, 0.01 in the first metatarsal axis and 0.0125 in the calcaneal axis. The results are expressed as means ± SD.

3. Results

The intraobserver and interobserver reliabilities for each measurement method and the post hoc power for interobserver reliability are shown in Tables 1–3. Regarding the talar axis, Method B yielded the best intraobserver and interobserver correlation coefficients (≥0.81) and showed satisfactory post hoc power. Regarding the first metatarsal axis, Method J yielded the best intraobserver and interobserver correlation coefficients (≥0.94), and Methods G, H and I showed very good results as well. Regarding the calcaneal axis, all the measurement methods showed very good results, but Method L provided the best intraobserver and interobserver correlation coefficients (≥0.95). Regarding the plantar axis, Method P, which used the horizontal plane (reference axis), was considered optimal; however, the intraobserver and interobserver correlation coefficients could not be calculated because all the values were zero. Regardless, Methods Q and R showed very good results for the plantar axis (data not shown).

Fig. 5 illustrates the measurement values obtained using the various measurement methods for each axis. The optimum measurement methods mentioned above generated the value of 21.5 ± 5.4° for the talar axis (Method B), 18.3 ± 3.9° for the first metatarsal axis (Method J), and 18.8 ± 5.2° for the calcaneal axis (Method L).

Moreover, when the optimum measurement methods mentioned above were applied, the value for the calcaneal pitch angle was 18.8 ± 5.2° when measured using Method L and Method P. The value for Meary's angle was calculated as −2.6 ± 6.6° when measured using Method B and Method J.

4. Discussion

This study revealed that a combination of the Shereff (Method L) [12] and horizontal plane (Method P) methods had the best reproducibility for measuring the calcaneal pitch angle, and a combination of the Shereff (Method B) [12] and Gould (Method J) [7] methods had the best reproducibility for measuring Meary's angle in the consecutive cases.

Regarding the talar axis, Method B yielded the best results for both the intraobserver and interobserver correlation coefficients. Compared to Method B, Method A had a similar interobserver correlation coefficient but a lower intraobserver correlation coefficient. The latter coefficient could be influenced by the observer's experience. The other

Table 1
Intraobserver and interobserver reliabilities of the talar axis, and post hoc power for interobserver reliability. The 95% confidence intervals are shown in parentheses.

	Method A	Method B	Method C	Method D	Method E	Method F
Intraobserver						
Observer 1	0.93 (0.88–0.96)	0.86 (0.78–0.92)	0.57 (0.40–0.73)	0.50 (0.32–0.67)	0.86 (0.78–0.92)	0.41 (0.22–0.60)
Observer 2	0.72 (0.58–0.83)	0.85 (0.76–0.91)	0.44 (0.25–0.63)	0.70 (0.56–0.82)	0.72 (0.57–0.83)	0.37 (0.17–0.57)
Observer 3	0.69 (0.54–0.81)	0.81 (0.70–0.89)	0.67 (0.52–0.79)	0.20 (0.0093–0.41)	0.73 (0.59–0.83)	0.65 (0.50–0.78)
Interobserver	0.81 (0.70–0.88)	0.83 (0.74–0.90)	0.34 (0.056–0.46)	0.30 (0.031–0.43)	0.75 (0.62–0.85)	0.52 (0.31–0.67)
Post hoc power	0.7504	0.8711	0	0	0.3146	0.0002

Table 2
Intraobserver and interobserver reliabilities of the first metatarsal axis, and post hoc power for interobserver reliability. The 95% confidence intervals are shown in parentheses.

	Method G	Method H	Method I	Method J	Method K
Intraobserver					
Observer 1	0.93 (0.88–0.96)	0.94 (0.90–0.96)	0.93 (0.89–0.96)	0.94 (0.91–0.97)	0.90 (0.84–0.94)
Observer 2	0.95 (0.92–0.97)	0.97 (0.96–0.99)	0.96 (0.94–0.98)	0.96 (0.93–0.98)	0.89 (0.82–0.93)
Observer 3	0.88 (0.80–0.93)	0.88 (0.82–0.93)	0.90 (0.84–0.94)	0.94 (0.90–0.97)	0.59 (0.42–0.74)
Interobserver	0.87 (0.80–0.93)	0.88 (0.81–0.93)	0.95 (0.91–0.97)	0.95 (0.92–0.97)	0.74 (0.59–0.83)
Post hoc power	0.9883	0.9951	1	1	0.2774

Table 3
Intraobserver and interobserver reliabilities of the calcaneal axis, and post hoc power for interobserver reliability. The 95% confidence intervals are shown in parentheses.

	Method L	Method M	Method N	Method O
Intraobserver				
Observer 1	0.99 (0.98–0.99)	0.99 (0.99–1)	0.87 (0.79–0.92)	0.85 (0.77–0.91)
Observer 2	0.99 (0.99–1)	0.98 (0.97–0.99)	0.99 (0.98–0.99)	0.95 (0.92–0.97)
Observer 3	0.98 (0.97–0.99)	0.98 (0.97–0.99)	0.98 (0.96–0.99)	0.87 (0.79–0.92)
Interobserver	0.95 (0.91–0.97)	0.95 (0.92–0.97)	0.98 (0.97–0.99)	0.91 (0.87–0.96)
Post hoc power	1	1	1	0.9999

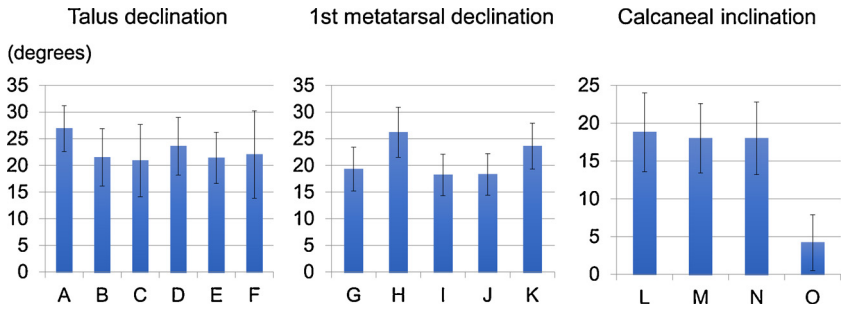

Fig. 5. Values obtained using various measurement methods for each axis.

methods (Methods C–F) yielded poor interobserver correlation coefficients. These results strongly suggest that the talar axis is most accurately and reliably determined using the lines tangent to the upper and lower surfaces (Method B), and all other definition methods are subject to low accuracy and poor reproducibility because of the difficulty of identifying the head, neck, and lateral process of the talus. Regarding the first metatarsal axis, Methods G–J displayed good correlation coefficients and post hoc analysis values, while Method K yielded the worst result. Method J is considered the preferable choice because it set the base of the first metatarsal and the centre of its head as landmarks and thus provided the best result, whereas the other methods used the diaphyseal end, which readily changes depending on its rotation. Regarding the calcaneal axis, Method L had the best intraobserver and interobserver correlation coefficients. Although Methods M, N, and O also had good correlation coefficients, Method L was considered most suitable because of the simplicity and reliability of determining the axis, as the tangent of the lower surface of the calcaneus, whereas the results of all other methods could potentially be impacted by deformations, such as bony spurs.

The values for each axis obtained using the optimal methods mentioned above were as follows: 21.5° for the declination of the talus, which was within the reported range of 14–36° using the Steel method [13] and coincided with the value of 21° reported by Weissman [22]; 18.3° for the declination of the first metatarsal, which was within the range of 16–30° reported using the Steel method; and 18.8° for the calcaneal base angle, which was within the ranges of 11–38° reported using the Steel method [13], 18–22° reported by Weissman [22], and 10–20° reported for healthy volunteers using the Gamble method [23]. All three of these axes were within reported standards, so they could be applied universally for consecutive cases. The values of the calcaneal pitch and Meary's angles obtained using the optimal methods mentioned above were as follows: 18.8° for the calcaneal pitch angle, which was slightly lower than the reported moderate range of 20–30° found with the Shereff method [12]; and −2.6° for the Meary's angle, which was within the range of −4 to 4° reported for neutral feet using the Gould method [7]. Both values tended to be slightly low, which could be attributed to the patient cohort comprising 75% women and a mean age of as high as 60.

Table 4 presents a summary of reports to date regarding the reliability of measurements assessing the calcaneal pitch angle and Meary's angle [11,15,20,24,25]. Regarding the method to set the talar axis, Younger et al. [15] referred to the report by Schon et al. [20]. Schon et al. [20] referred to the method of Gould (Method A); however, this method appears similar to Method D, as shown in the reported figure. The intraobserver and interobserver correlation coefficients have shown increasing trends in recent reports, which have used the angles between two axes to determine both the calcaneal pitch and Meary's angle. Comparatively high intraobserver and interobserver correlation coefficients were obtained in our measurements. However, our definition of Meary's angle differed from that in the literature, and the results could not be easily compared with those in the literature. In this study, the angle between the horizontal axis, which has a fixed value, and the single bone axis was utilized. The axes were well defined, and digital measurements were used, which ensured highly accurate values. Digital measurements have been reported to be more accurate than print measurements in radiographic measurements of feet [23]. The simple

Table 4
A summary of reports about the reliability of measurements assessing calcaneal pitch and Meary's angles.

		Method of axis establishment	Intraobserver/interobserver reliability	Value (Group)	Form (Film/ digital)
Schon et al. [20]	Calcaneal pitch angle	C: Method O P: Method R	0.82/0.76	Not available	Film
	Meary's angle	T: Method A (D) M1: Method K	0.71/0.59	Not available	
Younger et al. [15]	Calcaneal pitch angle	C: Method O P: Method R	0.68/0.76	8.4 ± 3.0° (Control) 4.0 ± 5.8° (Flatfoot)	Digital
	Meary's angle	T: Method A M1: Method K	0.75/0.83	7.1 ± 10.7° (Control) 21.1 ± 10.8° (Flatfoot)	
Ellis et al. [24]	Calcaneal pitch angle	C: Method O P: Method R	0.98/0.98	24.4 ± 6.9° (Control) 21.3 ± 5.9° (Mild flatfoot) 16.5 ± 5.7° (Severe flatfoot)	Digital
	Meary's angle	T: Method A M1: Method K	0.93/0.86	−0.7 ± 8.0° (Control) 4.2 ± 12.7° (Mild flatfoot) 21.8 ± 7.9° (Severe flatfoot)	
Sensiba et al. [11]	Calcaneal pitch angle	C: Method L P: Method P	0.98, 0.98, 0.93/0.948	Not available	Digital
	Meary's angle	T: Method A M1: Method J	0.93, 0.77, 0.83/0.781	Not available	
Arunakul et al. [25]	Calcaneal pitch angle	C: Method L P: Method P	0.95/0.98	23 ± 3° (Control) 14 ± 4° (Flatfoot) 27 ± 5° (Cavovarus)	Digital
	Meary's angle	T: Method A M1: Method K	0.96/0.69	2 ± 4° (Control) 18 ± 8° (Flatfoot) −10 ± 5° (Cavovarus)	
Present study (Applying the best reproducible methods)	Calcaneal pitch angle	C: Method L P: Method P	C: 0.99, 0.99, 0.98/0.95 P: not available	18.8 ± 5.2°	Digital
	Meary's angle	T: Method B M1: Method J	T: 0.86, 0.85, 0.81/0.83 M1: 0.94, 0.96, 0.94/0.95	−2.6 ± 6.6°	

C: calcaneus, P: plantar surface, T: talus, M1: 1st metatarsal.

manipulation for expansion, contraction and drawing of circles enables accurate measurement of the centre points and the horizontal line, which might be the reason for the high values obtained in this study. The measured values have been described by Younger et al. [15], Ellis et al. [24] and Arunakul et al. [25]. Although our method of axis establishment for calcaneal pitch angle was only consistent with that of Arunakul, the value of the calcaneal pitch angle was similar to those in the literature. Regarding Meary's angle, we referred to the Gould method, which originally defined measurements as negative values for the plantar angle [7], whereas all three previously mentioned reports recorded positive degrees for the plantar angle, as defined by Templeton et al. [14]. Standardization of the definitions will likely be necessary in the future. Additionally, our values of Meary's angle were also similar to those of Arunakul, even though their methods were different, and their interobserver reliability was low.

There are two limitations of this study. First, the validity of foot radiography is limited to some extent [26]. It has been reported that radiographic findings change substantially depending on the position of the hindfoot [5]. In actual clinical practice, it is important to comprehensively assess patients by physical examination and diagnostic imaging. Second, the present research only used the lateral radiographic images for evaluation. However, the lateral view has been reported to reflect clinical symptoms of flatfoot deformity better than the anteroposterior view on plain radiographs [20]. It has also been suggested that flatfoot symptoms are related to Meary's angle and the calcaneal pitch angle [15,27].

The present study elucidates the best reproducible measurements for radiographically assessing longitudinal tarsal axes in consecutive cases. This study can contribute to the standardization of assessing foot deformities.

Funding

Not applicable.

Role of the funding source

Not applicable.

Acknowledgements

Not applicable.

References

[1] Inui K, Ikoma K, Imai K, Ohashi S, Maki M, Kido M, et al. Examination of the correlation between foot morphology measurements using pedography and radiographic measurements. J Foot Ankle Surg 2017;56:298–303. https://doi.org/10.1053/j.jfas.2016.10.020.
[2] Aronson J, Nunley J, Frankovitch K. Lateral talocalcaneal angle in assessment of subtalar valgus: follow-up of seventy Grice-Green arthrodeses. Foot Ankle 1983;4:56–63. https://doi.org/10.1177/107110078300400202.
[3] Davids JR, Gibson TW, Pugh LI. Quantitative segmental analysis of weight-bearing radiographs of the foot and ankle for children: normal alignment. J Pediatr Orthop 2005;25:769–76. https://doi.org/10.1097/01.bpo.0000173244.74065.e4.
[4] Davis LA, Hatt WS. Congenital abnormalities of the feet. Radiology 1955;64:818–25. https://doi.org/10.1148/64.6.818.
[5] DiGiovanni JE, Smith SD. Normal biomechanics of the adult rearfoot: a radiographic analysis. J Am Podiatry Assoc 1976;66:812–24. https://doi.org/10.7547/87507315-66-11-812.
[6] Gamble F, Yale I. Clinical foot roentgenology. 2nd ed. New York, N.Y: Williams and Wilkins; 1975.
[7] Gould N. Graphing the adult foot and ankle. Foot Ankle 1982;2:213–9. https://doi.org/10.1177/107110078200200407.
[8] Lee KT, Kim KC, Park YU, Kim TW, Lee YK. Radiographic evaluation of foot structure following fifth metatarsal stress fracture. Foot Ankle Int 2011;32:796–801. https://doi.org/10.3113/FAI.2011.0796.
[9] Meary R. LE pied CREUX essentiel. [Etude Anatomo-Clinique]. Rev Chir Orthop Repar Appar Mot 1967;53:390–410. [in French].
[10] Okuda R, Kinoshita M, Yasuda T, Jotoku T, Kitano N, Shima H. The shape of the

lateral edge of the first metatarsal head as a risk factor for recurrence of hallux valgus. J Bone Jt Surg Am 2007;89:2163–72. https://doi.org/10.2106/JBJS.F.01455.
[11] Sensiba PR, Coffey MJ, Williams NE, Mariscalco M, Laughlin RT. Inter- and intraobserver reliability in the radiographic evaluation of adult flatfoot deformity. Foot Ankle Int 2010;31:141–5. https://doi.org/10.3113/FAI.2010.0141. Pubmed:20132751.
[12] Shereff MJ. Radiographic analysis of the foot and ankle. In: Shereff MJ, editor. Disorders of the foot and ankle. Philadelphia, PA: WB Saunders; 1991. p. 100–2.
[13] Steel 3rd MW, Johnson KA, DeWitz MA, Ilstrup DM. Radiographic measurements of the normal adult foot. Foot Ankle 1980;1:151–8. https://doi.org/10.1177/107110078000100304.
[14] Templeton AW, McAlister WH, Zim ID. Standardization of terminology and evaluation of osseous relationships in congenitally abnormal feet. Am J Roentgenol Radium Ther Nucl Med 1965;93:374–81.
[15] Younger AS, Sawatzky B, Dryden P. Radiographic assessment of adult flatfoot. Foot Ankle Int 2005;26:820–5. https://doi.org/10.1177/107110070502601006.
[16] Kido M, Ikoma K, Imai K, Maki M, Takatori R, Tokunaga D, et al. Load response of the tarsal bones in patients with flatfoot deformity: in vivo 3D study. Foot Ankle Int 2011;32:1017–22. https://doi.org/10.3113/FAI.2011.1017.
[17] Ikoma K, Ohashi S, Maki M, Kido M, Hara Y, Kubo T. Diagnostic characteristics of standard radiographs and magnetic resonance imaging of ruptures of the tibialis posterior tendon. J Foot Ankle Surg 2016;55:542–6. https://doi.org/10.1053/j.jfas.2016.01.009.
[18] Coughlin MJ, Saltzman CL, Anderson RB. Mann's surgery of the foot and ankle. 9th ed. Philadelphia: Elsevier, Saunders; 2011.
[19] Lee KM, Chung CY, Park MS, Lee SH, Cho JH, Choi IH. Reliability and validity of radiographic measurements in hindfoot varus and valgus. J Bone Jt Surg Am 2010;92:2319–27. https://doi.org/10.2106/JBJS.I.01150.
[20] Schon LC, Weinfeld SB, Horton GA, Resch S. Radiographic and clinical classification of acquired midtarsus deformities. Foot Ankle Int 1998;19:394–404. https://doi.org/10.1177/107110079801900610.
[21] Altman DG. Practical statistics for medical research. New York, N.Y: Chapman & Hall; 1991.
[22] Weissman SD. Radiology of the foot. 2nd ed. New York, N.Y: Williams & Wilkins; 1989. p. 72–3.
[23] Farber DC, Deorio JK, Steel MW. Goniometric versus computerized angle measurement in assessing hallux valgus. Foot Ankle Int 2005;26:234–8. https://doi.org/10.1177/107110070502600309.
[24] Ellis SJ, Yu JC, Williams BR, Lee C, Chiu YL, Deland JT. New radiographic parameters assessing forefoot abduction in the adult acquired flatfoot deformity. Foot Ankle Int 2009;30(December (12)):1168–76. https://doi.org/10.3113/FAI.2009.1168.
[25] Arunakul M, Amendola A, Gao Y, Goetz JE, Femino JE, Phisitkul P. Tripod index: a new radiographic parameter assessing foot alignment. Foot Ankle Int 2013;34(October (10)):1411–20. https://doi.org/10.1177/1071100713488761.
[26] Perry MD, Mont MA, Einhorn TA, Waller JD. The validity of measurements made on standard foot orthoroentgenograms. Foot Ankle 1992;13:502–7. https://doi.org/10.1177/107110079201300902.
[27] Pehlivan O, Cilli F, Mahirogullari M, Karabudak O, Koksal O. Radiographic correlation of symptomatic and asymptomatic flexible flatfoot in young male adults. Int Orthop 2009;33:447–50. https://doi.org/10.1007/s00264-007-0508-5.